American Mineralogist, Volume 70, pages 1193–1204, 1985

Coexisting paragonite–phengite in blueschist eclogite: a TEM study[1]

JUNG HO AHN, DONALD R. PEACOR, AND ERIC J. ESSENE

Department of Geological Sciences
The University of Michigan
Ann Arbor, Michigan 48109

Abstract

Coexisting paragonite and phengite in an eclogite from the Franciscan Formation at Cazadero, California, were studied by transmission electron microscopy. The phengites are characterized by high Fe + Mg (0.48 per 2 octahedral cations) and Si (3.21 per 4 tetrahedral cations). The phengite has 15 mole% Na substituting for K, and the paragonite has 7 mole% K substituting for Na.

Half-micron sized lamellae of phengite were observed intergrown in paragonite, but not vice versa. Phengite is predominantly a well-ordered $2M_1$ polytype almost free of stacking disorder, except for phengite lamellae intergrown within paragonite. However, paragonite is highly imperfect, with stacking disorder and a high density of edge dislocation-like features. Paragonite shows stacking disorder originating from random layer rotations of n(120°) and also exhibits complex polytypism. Although most paragonite is a $2M_1$ polytype, there are locally random intercalations of a 3-layer polytype. In addition, the 2-layer and 3-layer polytypes are intercalated in an ordered fashion resulting in an 8-layer polytype composed of a 2-layer and two 3-layer subunits. Phengite is locally deformed below optical microscopic resolution and shows complex bending and kinking.

Introduction

Coexisting paragonite and muscovite have been observed in eclogite by many investigators (Essene, 1967; Ernst, 1976; Ernst and Dal Piaz, 1978; Holland, 1979; Feininger, 1980; Krogh, 1980; Oberhänsli, 1980; Heinrich, 1982). Rosenfeld et al. (1958) and Zen and Albee (1964) have shown that the basal spacings of the coexisting muscovite and paragonite pairs change progressively with increase in metamorphic grade and therefore indirectly with temperature.

The solid solution series muscovite ($KAl_2Si_3AlO_{10}(OH)_2$)–celadonite ($KR^{2+}R^{3+}Si_4O_{10}(OH)_2$), where R^{2+} is Mg^{2+} and Fe^{2+}, and R^{3+} is Al^{3+} and Fe^{3+}, was discussed by Schaller (1950) and Foster (1956). Phengite is a dioctahedral mica that deviates from the ideal muscovite composition toward $K(Al_{1.5}R^{2+}_{0.5})(Si_{3.5}Al_{0.5})\ O_{10}(OH)_2$ (Bailey, 1980). The amount of phengitic substitution is a function of pressure and temperature, although bulk rock composition may also be significant (Ernst, 1963; Velde, 1965b, 1967; Brown, 1968; Powell and Evans, 1983).

Phengite commonly occurs in metamorphic rocks, but paragonite is rare compared to phengite. The rarity of paragonite was explained by Guidotti (1968) on the basis of compositional control and stability relations, and he suggested that the presence of paragonite is related to relative enrichment in Al_2O_3 and/or $NaAlO_2$ in low- to medium-grade metamorphic rocks. Rocks with highly aluminous minerals such as chloritoid, kyanite, etc., commonly have paragonite, whereas less aluminous rocks that contain biotite rarely have paragonite. Some of the apparent scarcity of paragonite is due to the difficulty with its identification (Guidotti, 1968). In addition, paragonite is unstable in the presence of K-feldspar and with potassic solutions because it will react to form muscovite + albite. At higher temperatures muscovite can accept a larger paragonite component than vice versa (Burnham and Radoslovich, 1964), and this also reduces the likelihood of finding paragonite. Nevertheless, the occurrence of coexisting paragonite and phengite remains interesting because of the solvus relations (Eugster, 1956; Eugster et al., 1972; Blencoe and Luth, 1973) and because it offers potential as a geothermometer once the solvus is accurately defined.

Essene (1967) reported coexisting paragonite and phengite in blueschist ecologite (Univ. of Calif., Berkeley, No. 665-C19) from the Franciscan Formation at Cazadero, California. These white micas were present in the gneissic layers lacking in glaucophane and rich in omphacite. During analysis of paragonite and phengite by electron microprobe, a step scan across both minerals for Na, K and Ca showed intermediate values (Essene, 1967). These intermediate values can be explained by three possibilities: (1) fine grained intergrowths of both micas below electron microprobe resolution ($<2\ \mu m$); (2) the presence of mixed-layering (Zen and Albee, 1964; Albee and Chodos, 1965;

[1] Contribution No. 402 from the Mineralogical Laboratory, Department of Geological Sciences, The University of Michigan, Ann Arbor, Michigan 48109.

0003–004X/85/1112–1193$02.00

Table 1. Electron microprobe analyses of coexisting paragonite (Pa) and phengite (Ph)

Oxide weight percent			Atoms / 6 (IV+VI) cation		
	Ph	Pa		Ph	Pa
SiO_2	47.55	46.43	Si	3.21	3.02
Al_2O_3	28.73	37.48	Al(IV)	0.79	0.98
TiO_2	0.36	0.10	Al(VI)	1.49	1.88
Cr_2O_3	0.03	0.09	Ti	0.02	0.01
Fe_2O_3	5.04[1]	1.72[1]	Cr	0.00	0.00
FeO	0.00[1]	0.20[1]	Fe^{3+}	0.25[1]	0.08[1]
MnO	0.10	0.01	Fe^{2+}	0.00[1]	0.01[1]
MgO	2.30	0.16	Mn	0.01	0.00
CaO	0.02	0.14	Mg	0.23	0.02
Na_2O	1.15	7.25	Ca	0.00	0.01
K_2O	9.68	0.88	Na	0.15	0.91
H_2O	4.51[2]	4.62[2]	K	0.83	0.07
F_2	0.00	0.00	OH	2.03[2]	2.00[2]
Sum	99.47	99.11	O	9.97[2]	10.00[2]

[1] Fe^{2+} and Fe^{3+} calculated to yield a charge of +22 on an anhydrous basis.

[2] H_2O calculated from the OH necessary to fill the anion sites.

Frey, 1969); (3) the presence of variable amounts of exsolved micas (for example, Veblen, 1983a).

In this paper transmission electron microscopy (TEM) and X-ray analytical electron microscopy (AEM) techniques were used to investigate the nature of coexisting paragonite and phengite in blueschist eclogite at high resolution in order to determine the detailed chemical and structural relations and to determine the origins of intermediate values for Na and K observed with the electron microprobe (Essene, 1967). This study was also prompted by a general question regarding the nature of phengite: are the divalent and trivalent components in these phengites homogeneously distributed within the individual layers of mica structure or are the divalent components concentrated in individual layers or packets of layers that are too small to be resolved even by X-ray diffraction?

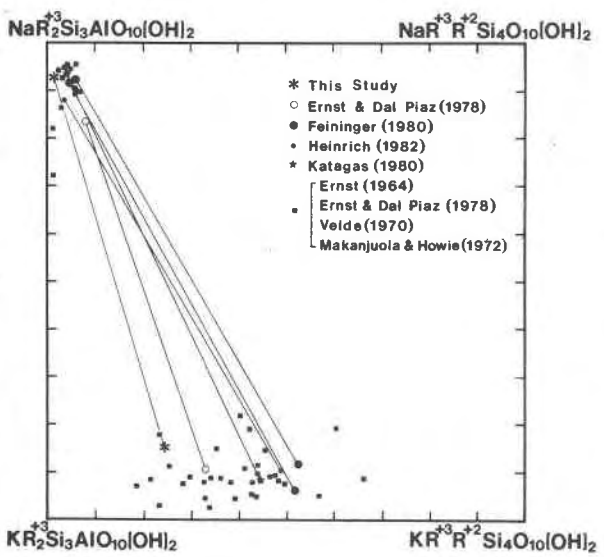

Fig. 1. Composition diagram showing celadonitic substitution and mutual paragonite and phengite substitutions. Tie lines indicate coexisting paragonite–phengite pairs, and other data are derived from literature values for eclogites and blueschists.

Experimental

The specimen observed in this study is from a gneissic Type IV blueschist eclogite from the Franciscan Formation at Cazadero, California (Coleman and Lee, 1963), and was previously studied by Essene (1967). Samples were first prepared as polished thin sections for petrographic observation and electron microprobe analysis. The surfaces of thin sections were cut perpendicular to the gneissic layers to obtain optimum orientation for lattice fringe images in TEM observations. Following optical observation and electron microprobe analysis, washers were attached to selected areas, and after detaching from the slide these washer-mounted samples were thinned in an ion mill and then lightly carbon-coated. The electron microscope used is the University of Michigan JEOL JEM-100CX instrument fitted with a solid state detector for energy dispersive analysis. AEM techniques are described in detail in Blake et al. (19809 and Blake and Peacor (1981). All TEM observations were performed and interpreted using the theory described by Iijima and Buseck (1978); only one-dimensional lattice fringe images are obtained by using the (00*l*) reflections.

Composition of paragonite and phengite

Coexisting paragonite and phengite are observed in gneissic layers that consist of epidote–glaucophane–garnet domains complexly intergrown with sodic pyroxene (om-

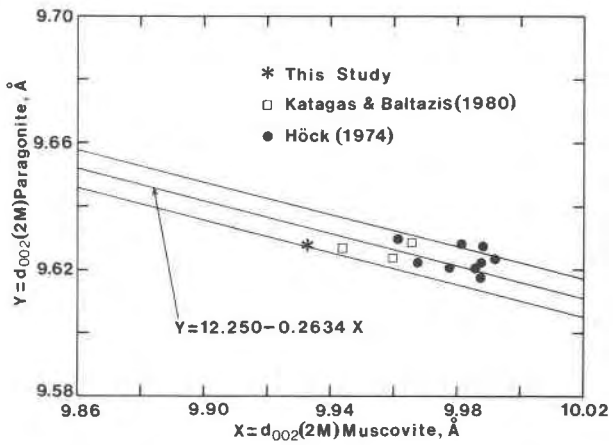

Fig. 2. Basal spacings of coexisting paragonite and phengite. The central straight line corresponds to the regression line: $d(002)$ 2M paragonite = 12.250 − 0.264 $d(002)$ 2M muscovite (after Zen and Albee, 1964). The two supplementary lines indicate the uncertainty limits of Zen and Albee. Other data from the literature are plotted for comparison.

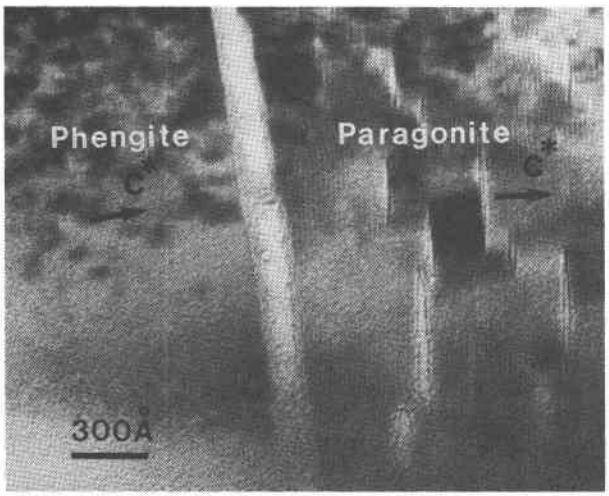

Fig. 3. Low magnification TEM image of a grain boundary between paragonite and phengite. Thin sample area of paragonite shows splitting along layers due to beam damage; phengite does not exhibit this feature.

phacite zoned to acmite–jadeite)–garnet–quartz–albite domains. The sodic pyroxenes in this sample were analyzed by Essene and Fyfe (1967), and the garnets were analyzed by Dudley (1969).

Paragonite is rare in the Franciscan Formation, and only three paragonite localities were found by Essene (1967) from an X-ray powder diffraction search of more than 200 specimens of white micas. Paragonite may be limited to basic rocks of a restricted composition as Banno (1964) suggested for Japanese glaucophane schists. On the other hand, many eclogitic rocks from New Caledonia contain paragonite (Black, 1975).

Coexisting paragonite–phengite pairs were analyzed using the electron microprobe (Table 1). These analyses are generally in reasonable agreement with the older data of Essene (1967). The analyses reveal an asymmetric solvus between paragonite and phengite, with a 15 mole% paragonite component ($NaAl_2Si_3AlO_{10}(OH)_2$) in phengite and a 7 mole% muscovite component ($KAl_2Si_3AlO_{10}(OH)_2$) in paragonite (Fig. 1). The phengite analyses display a high phengitic substitution (Si = 3.21) when the chemical formula is normalized to 6 octahedral and tetrahedral cations. Charge balance considerations suggest that most of the iron is ferric (Table 1), but this result is imprecise due to analytical errors and to assumptions made in normalization. However, Ernst (1964) and Makanjuola and Howie (1972) observed that ferric iron is dominant in white micas from blueschist facies. Our phengite analysis can be recast approximately as 15% paragonite, 46% celadonite, 12% ferrimuscovite, and only 27% muscovite. The coexisting paragonite shows little excess Si (Table 1). The analytical data on coexisting paragonite and phengite have been plotted on a composition diagram showing celadonite substitution in comparison with other data from eclogite and blueschist rocks (Fig. 1). It can be seen that paragonite contains a small celadonite component (< 10%) even when coexisting with celadonite-rich phengites. The scattered data lying inside the tielines connecting coexisting pairs suggest that these white micas formed at higher temperatures or contain submicroscopic intergrowths of other micas. Submicroscopic intergrowth of phengite within paragonite was observed in this study, and it will be discussed in a later section.

Several experimental studies attempting to define the paragonite–muscovite solvus have been carried out (Eugster and Yoder, 1955; Iiyama, 1964; Nicol and Roy, 1965; Popov, 1968; Eugster et al., 1972; Blencoe and Luth, 1973). However, the solvus is still not tightly constrained by compositional reversals. The experiments show that there is an increasing amount of Na in muscovite and K in paragonite with increasing temperature and that the solvus is asymmetric in that there is less solid solution in paragonite than

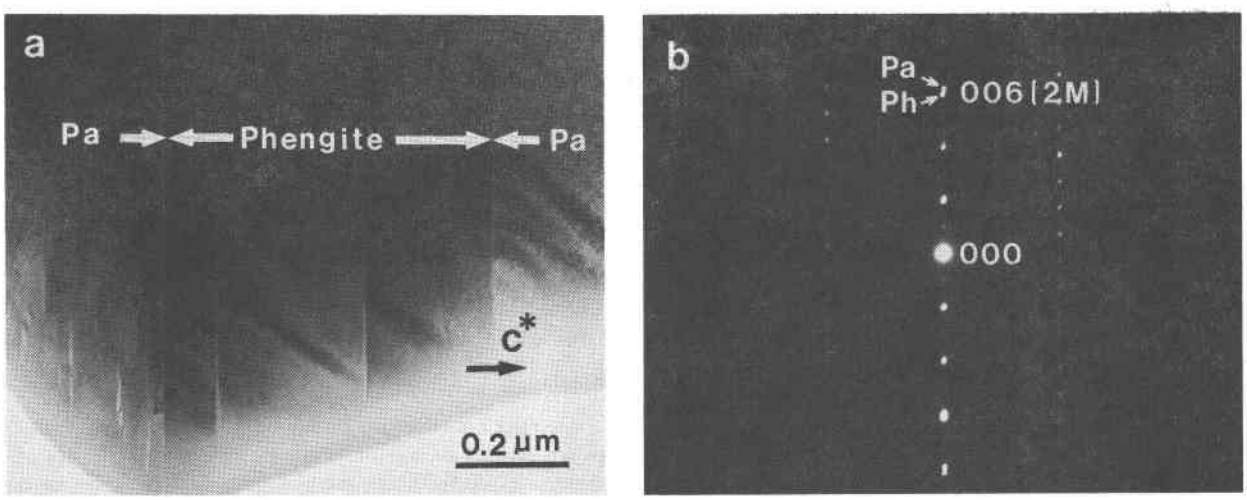

Fig. 4. (a) Low magnification electron micrograph of an intergrowth of phengite lamellae (0.6 µm width) within paragonite (Pa), and (b) electron diffraction pattern from this area showing split diffractions from phengite (Ph) and paragonite (Pa).

in muscovite. This asymmetric solid solution relationship is explained by Burnham and Radoslovich (1964) through a consideration of the variation of alkali-oxygen interatomic distances with varying K/Na atomic ratio. They pointed out that substitution of Na for K does not result in a linear variation of the alkali-oxygen bond distances. The bond-length changes as Na replaces K are small and gradual, whereas they are large when K replaces Na.

Basal spacings of coexisting paragonite and phengite

Zen and Albee (1964) suggest that the basal spacings of coexisting muscovite–paragonite fit the regression equation:

$$d(002)2M\ Pg = 12.250 - 0.2634\ d(002)2M\ Mu \pm 0.0006Å$$

on the basis of the results for 42 coexisting muscovite and paragonite pairs from various metamorphic rocks. They pointed out that the basal spacings of the coexisting muscovite and paragonite change progressively according to the grade of metamorphism, so these parameters provide a sensitive and continuous measure of changing metamorphic grade.

Basal spacings of the paragonite and phengite of this study were measured with powder X-ray diffraction, using the $(006)_{2M}$ reflections with quartz as an internal standard. The basal spacings of the paragonite and phengite are 9.628Å and 9.933Å and fall below the regression line of Zen and Albee (Fig. 2). Zen and Albee (1964) explained the scatter in values by several causes: (1) only partial or total lack of attainment of chemical equilibrium between the two micas; (2) the presence of different mica polymorphs; (3) the presence of mixed-layering; and (4) the presence of other components in the micas. Among the several factors given by Zen and Albee, the most important one is the effect of other components, especially the phengite component. Radoslovich and Norrish (1962) showed that the basal spacing varies with the compositions of the octahedral sites, and Ernst (1963) pointed out that phengitic substitution leads to abnormally small basal spacings in muscovite. Low basal spacings due to phengitic subsitution have been observed by many workers (e.g., Ernst, 1963; Cipriani et al., 1968; Chiesa et al., 1972; Höck, 1974; Katagas and Baltatzis, 1980). The substitutions as shown by the analytical data of Table 1 therefore serve to explain the deviation of the $d(002)$ values from the trend of Zen and Albee.

Electron microscopic observations

Because of the relatively small difference in basal spacings of paragonite and phengite (9.63 and 9.93Å, respectively), lattice fringe images of both are almost identical. The contrast in TEM images is also very similar for both. It is therefore very difficult to differentiate between these micas directly from TEM images. However, we distinguished the micas by using electron diffraction patterns that exhibited splitting of $00l$ reflections and by using X-ray analytical electron microscopic techniques. The only

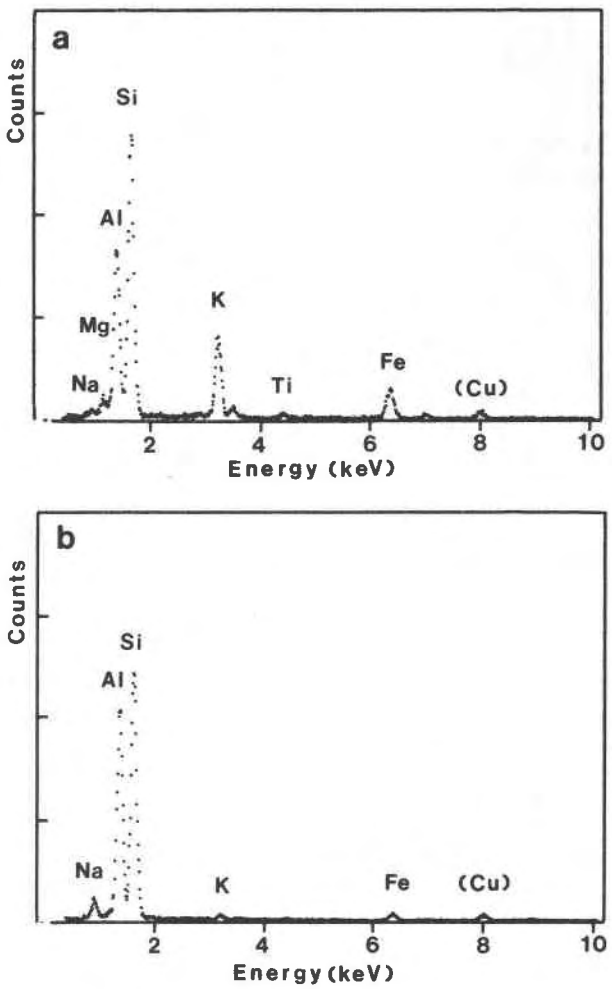

Fig. 5. Energy dispersive X-ray spectra of the phengite (a) and paragonite (b). Small Cu peaks are present in both spectra due to contamination.

significant difference that can be observed directly in ordinary bright field images of individual phases is their different stabilities under the electron beam. Both paragonite and phengite are relatively unstable, and both display a "mottled" image appearance due to beam damage but paragonite is damaged much faster than phengite and shows a different resultant texture; paragonite splits along layers, eventually exhibiting lenticular layer separations in areas of thin edges (Fig. 3). Those lenticular fissures are a beam-damage feature of paragonite caused by rapid volatilization or diffusion of interlayer Na (Ahn and Peacor, unpublished data).

Paragonite–phengite intergrowth

Phengite lamellae are occasionally observed to be intergrown within paragonite grains as packets of layers approximately 0.5–0.8 μm thick. Figure 4a represents an example of typical phengite lamellae intergrown within paragonite grains. The thin edges of paragonite show the

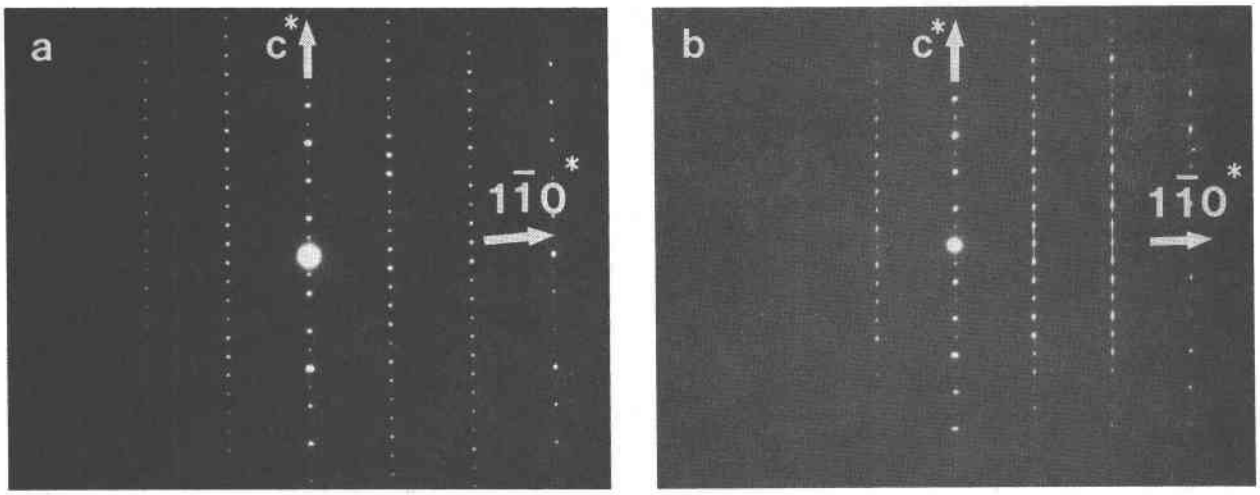

Fig. 6. (a) Electron diffraction pattern of phengite. Phengite shows no streaking parallel to **c***. (b) Electron diffraction pattern from paragonite showing diffuse streaking along rows of reciprocal lattice points with $k \neq 3n$. 110* refers to the reciprocal lattice direction [110].

characteristic lenticular splitting caused by beam damage. Electron diffraction patterns (Fig. 4b) show that the 00*l* reflections are two separate reflections, indicating that the area within the beam is composed of two intergrown micas that have different basal spacings. Qualitative X-ray analytical electron microscopy also confirms that phengite is intergrown with paragonite (Fig. 5a, b). The X-ray spectrum from phengite (Fig. 5a) shows a significant Mg and Fe content and high K whereas the spectrum from paragonite (Fig. 5b) shows a low Mg, Fe content and low K. No significant chemical difference between fine scale intergrown phengite and large grains of phengite was observed.

This kind of fine scale intergrowth of different micas below electron microprobe resolution may be a common feature in both naturally occurring and synthetic micas. If such intergrown micas are analysed and assumed to be single phases serious errors in the chemical compositions may result. In order that solid solution relationships in micas may be accurately defined, it is essential that the presence of such intergrowths be recognized and characterized.

Structural imperfections in paragonite

At the beginning of our TEM study, the structure of phengite was expected to be more imperfect than that of paragonite, because phengite has a high degree of (Fe, Mg) substitution, possibly resulting in local strain and/or domains of enrichment of (Fe, Mg) and Si. Our results are contrary to these predictions, however, in part as demonstrated in the electron diffraction pattern of phengite which shows no effects of stacking disorder. Figure 6a is an electron diffraction pattern from $2M_1$ phengite and shows only sharp, well-defined reflections, indicating that phengite has an ordered stacking sequence. However, the electron diffraction patterns of paragonite imply stacking disorder and complex polytypism. We will discuss the aspects of polytypism of paragonite and phengite in detail in a later section, but we note here that many paragonite grains give electron diffraction patterns similar to those shown in Figure 6b; these display diffuse streaking along **c*** in all reciprocal lattice rows with $k \neq 3n$. Such streaking indicates that stacking disorder is principally due to random layer rotations of n(120°) in layer stacking sequences. This kind of stacking disorder is most common in phyllosilicates (Smith and Yoder, 1956; Brown and Bailey, 1962; Ross et al., 1966), and has been observed, for example, in biotite (Iijima and Zhu, 1982) and in chlorite (Schreyer et al., 1982; Veblen, 1983b; Ahn and Peacor, 1985) using electron diffraction patterns.

Edge dislocation-like features are another type of structural imperfection shown in paragonite (Fig. 7). They appear to consist simply of the termination of an entire

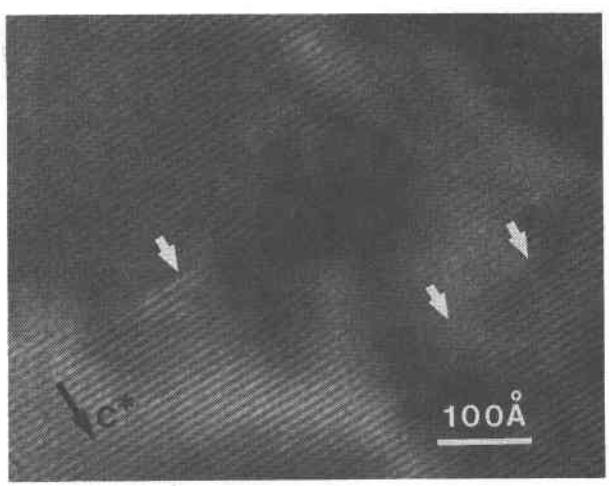

Fig. 7. Lattice fringe image of paragonite showing edge dislocation-like features (indicated by arrows).

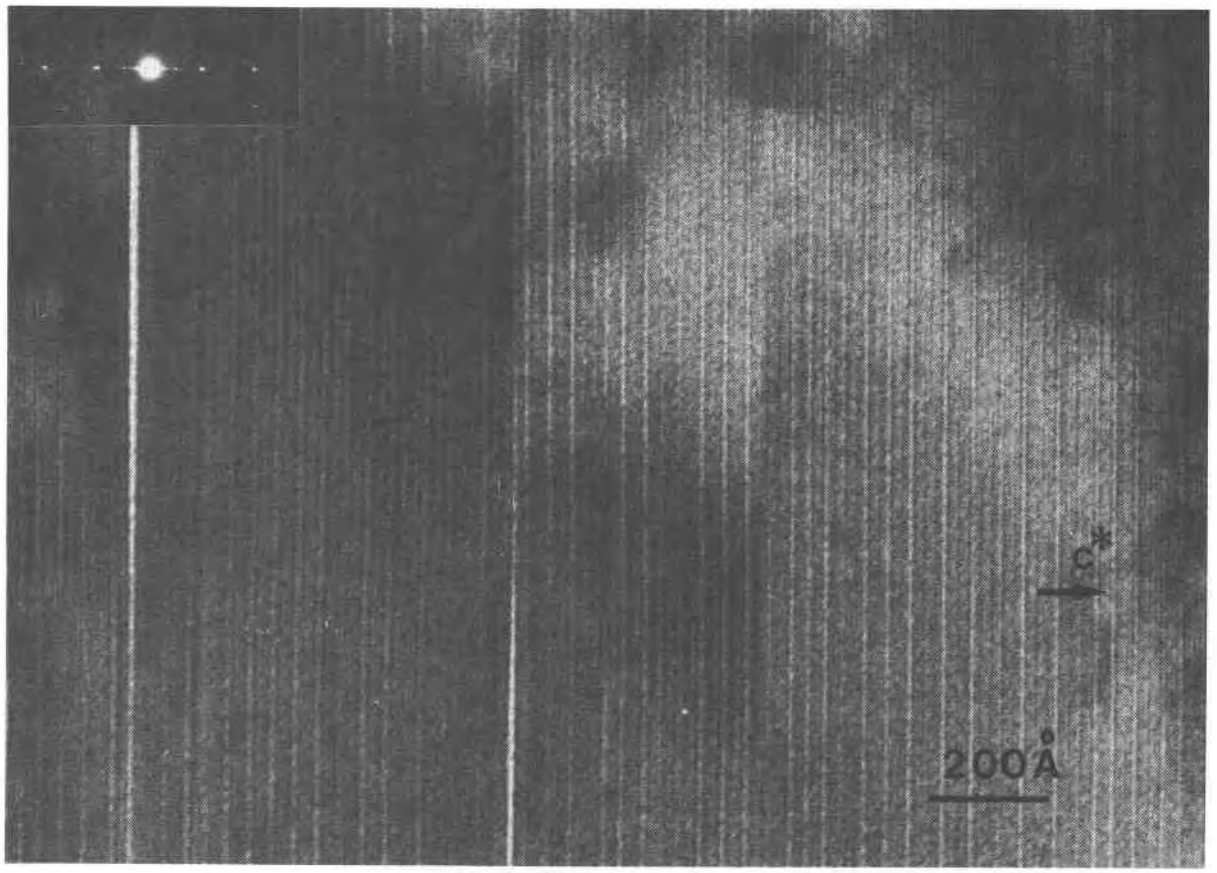

Fig. 8. Lattice fringe image showing complex stacking sequences in phengite which is intergrown with paragonite. 4- and 2-layer periodicities are dominant, but 3-layer or disordered sequences are also present.

structure layer. Such edge dislocations have been more frequently observed in 2:1 layer silicates (see, Veblen and Buseck, 1980, Fig. 13; Veblen and Buseck, 1981, Fig. 19c; Lee et al., 1985, Fig. 1b) relative to 1:1 layer silicates and chlorites.

Throughout our observation of phengite (which contains significant Fe and Mg) we did not observe intercalated extra brucite-like layers which would serve to locally form a chlorite-like structure. Such interlayering of extra brucite-like layers is commonly observed as a planar defect in trioctahedral 2:1 layer silicates (Veblen, 1980, 1983b; Veblen and Buseck, 1979, 1981; Iijima and Zhu, 1982;

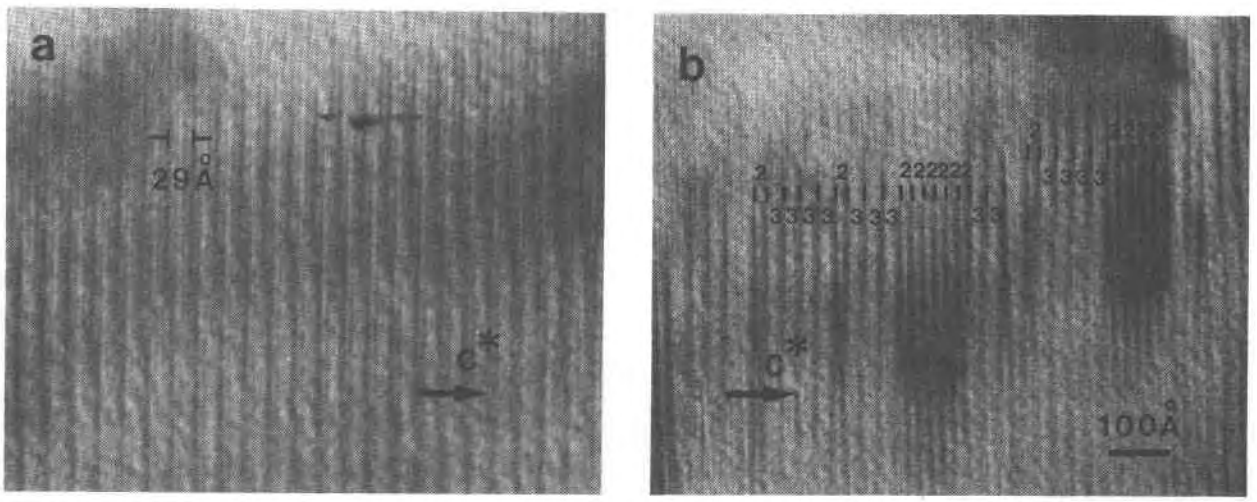

Fig. 9. (a) Lattice fringe image of 3-layer paragonite; (b) Lattice fringe image of randomly interlayered 2-layer and 3-layer paragonite.

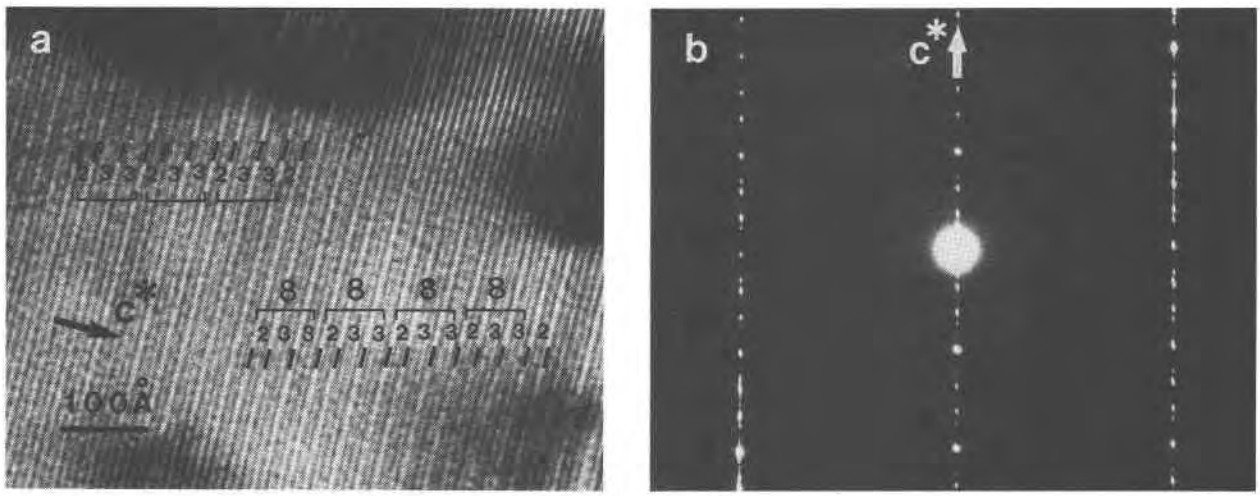

Fig. 10. (a) Lattice fringe image of paragonite showing an 8-layer polytype, consisting of a 3-layer, 3-layer, 2-layer sequence; (b) Electron diffraction pattern from 8-layer paragonite.

Veblen and Ferry, 1983; Olives Baños et al., 1983; Yau et al., 1984). We also did not observe any direct evidence for concentration of Fe and Mg into trioctahedral layers, which would result in localized units of biotite.

Polytypism of paragonite and phengite

Polytypism in mica has long been of interest to mineralogists and metamorphic petrologists. The six simplest mica polytypes were described by Smith and Yoder (1956), and Ross et al. (1966) carried out a systematic generation of all possible mica polytypes with layer repeats up to six. Baronnet (1975) rationalized complex polytypism on the basis of a spiral growth mechanism. Güven and Burnham (1967) compared the unit layers of a $2M_1$ and 3T muscovite, and observed that: (1) cations are partially ordered in both tetrahedral and octahedral sites in 3T, whereas in the $2M_1$ muscovite the distribution of Si and Al in tetrahedral sites appears to be completely disordered, and (2) the 3T unit layer possesses space group symmetry $C2$, whereas the $2M_1$ muscovite layer has space group $C\bar{1}$. The causes of structural control of polytypism, if any, are still not clear. Güven (1971) suggested that the polytypic sequence is determined by the distortion in single layers through cation substitutions or ordering. However, Takeda and Ross (1975) compared the crystal structures of coexisting 1M and $2M_1$ biotite and proposed an origin for biotite polytypism due to different atomic and geometric constraints imposed upon the unit layer by adjacent layers. Thermodynamic consequences of mica polytypism are still unclear (Velde, 1965a), but Liborio and Mottana (1975) suggest that 3T polytypes are favored in high pressure, low temperature metamorphic conditions and with a pure H_2O fluid that is free of CO_2. The large number of polytypes found in biotite (Ross et al., 1966; Iijima and Buseck, 1978) and in paragonite and phengite (this study) suggest that non-equilibrium factors such as growth mechanisms or variable stress may be controlling factors in determining mica polytypes. In addition, data by Stöckhert (1985) indicate that high values of the ratio Mg/(Al + Fe + Mg) are correlated with the 3T polytype of phengite. Recently there have been several detailed studies of mica polytypism using high resolution transmission electron microscopy (HRTEM) (Iijima and Buseck, 1978; Amouric et al., 1981; Amouric and Baronnet, 1983), but the causes of polytypic differences remain unclear.

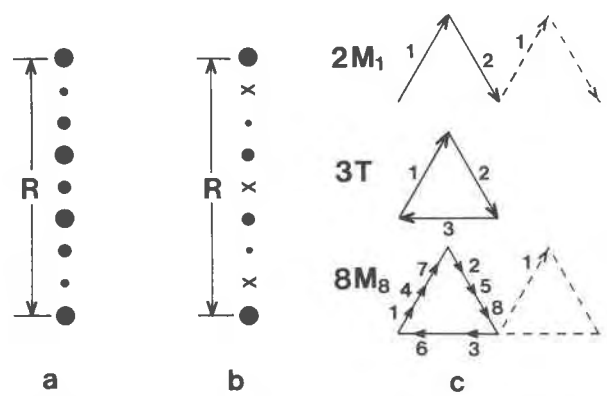

Fig. 11. (a) Representation of the periodic intensity distribution of $8M_8$ biotite polytypes (from Ross et al., 1966). The distance R represents the single-layer repeat of 10Å; (b) Schematic representation of the electron diffraction pattern of Figure 10b for the 8-layer paragonite. The crosses correspond to very weak reflections; (c) The stacking sequence of $2M_1$, 3T, and $8M_8$ polytypes as represented by a Smith-Yoder diagram (from Ross et al., 1966).

Most white micas of metamorphic rocks are $2M_1$ and 1M polytypes, with occasional 3T polytypes. Liborio and Mottana (1975) reported occurrences of 3T white micas and discussed their conditions of formation in light of the local geological relationships and metamorphic environments. In addition, Frey et al. (1983) reported regional distribution of white K-mica polytypes from the Central Alps, and they found that the phengite content of white micas is related to metamorphic grade but does not control the 3T

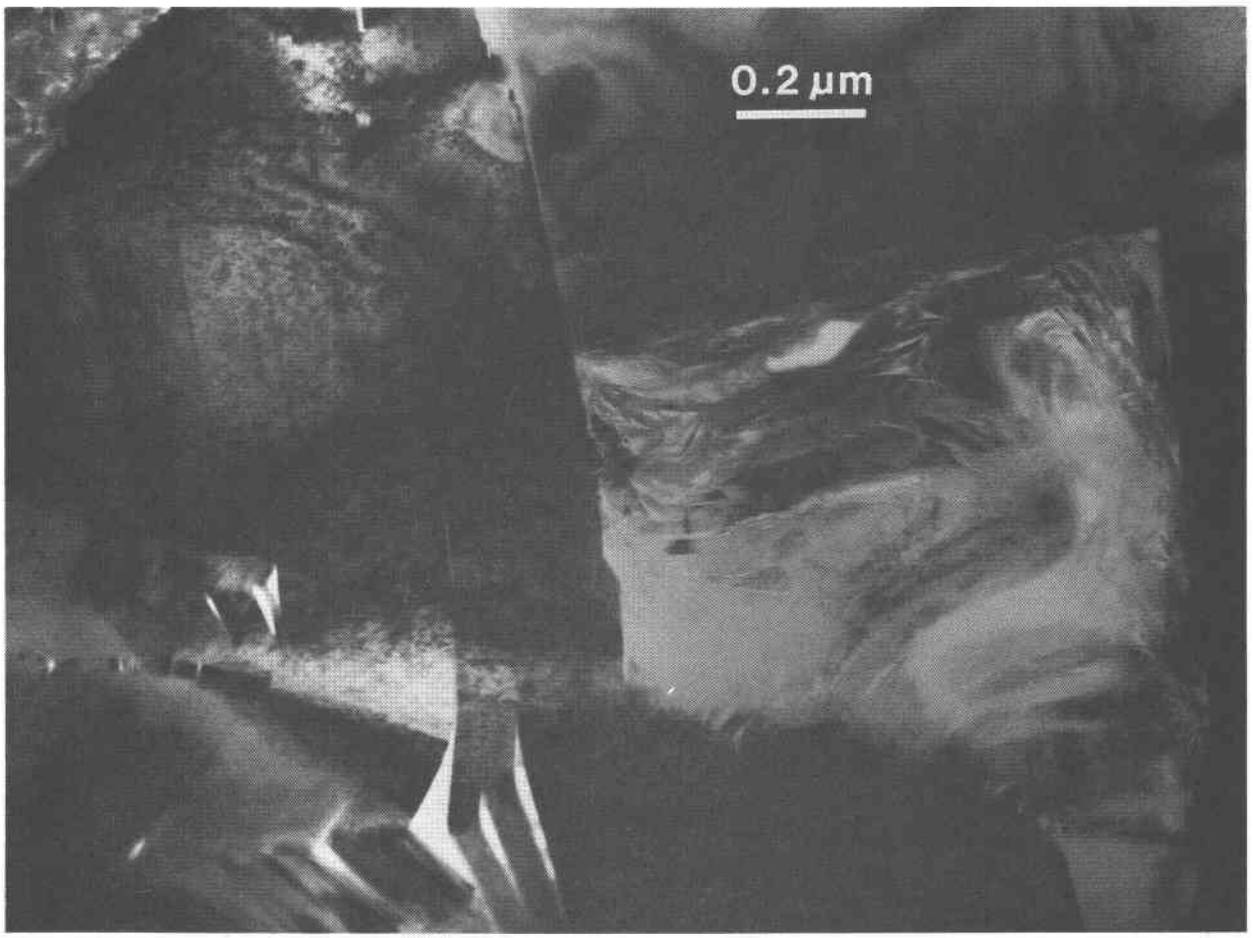

Fig. 12. Severely deformed phengite. Phengite layers are bent and split into chevron folds.

mica stability. Most 3T white micas usually coexist with $2M_1$ polytypes. The $2M_2$ polytype is rare in dioctahedral micas, and is primarily found in Li-bearing micas (see, Ross et al., 1966; Bailey, 1980). In our study both phengite and paragonite were found to be primarily $2M_1$ micas through single crystal X-ray diffraction data, but both micas were found to have variations in polytypic sequence when examined by TEM. The large phengite crystals occur consistently as only the $2M_1$ polytype and are almost entirely free of stacking disorder as shown by electron diffraction patterns (Fig. 6a). However, phengites intergrown with paragonite at the half-micron scale do show variable periodicity as shown in Figure 8. In this electron micrograph various kinds of apparent periodicities are shown; 4- and 2-layer periodicities are most abundant but there are also apparent 3-layer or disordered stacking sequences. Electron diffraction patterns of this area show heavy streaking parallel to **c***.

When comparing paragonite to phengite, paragonite is seen to exhibit more complex polytypism even though the $2M_1$ polytype is dominant in paragonite. Besides the $2M_1$ polytype, paragonite crystals occasionally consist of a well-ordered 3-layer polytope (Fig. 9a). The 2-layer and 3-layer paragonite polytypes are intergrown randomly in units from tens of Angstroms to hundreds of Angstroms in thickness, occasionally showing one unit of 2-layer polytypes intercalated in 3-layer polytype regions and vice versa (Fig. 9b). This kind of complex interlayering of different mica polytypes has only been observed in biotite (Iijima and Buseck, 1978). Furthermore, these 2-layer and 3-layer polytypes were found in one paragonite grain to be ordered in a 1 to 2 ratio producing an 8-layer superlattice consist of a 2-layer, 3-layer and 3-layer stacking sequence. Figures 10a and 10b show such 8-layer polytype lattice fringe images and the equivalent selected-area electron diffraction pattern. They are repeated over a substantial range, although an extra 2-layer unit is shown interrupting the regular 8-layer sequence (Fig. 10a). The $8M_8$ polytype for biotite, which consists of the stacking sequence 3T, 3T and $2M_1$, was reported by Ross et al. (1966), who showed the periodic diffraction intensity distribution and a schematic diagram of the stacking sequence (Fig. 11). The electron diffraction pattern from 8-layer paragonite (Fig. 10b) agrees to a first approximation with the calculated periodic inten-

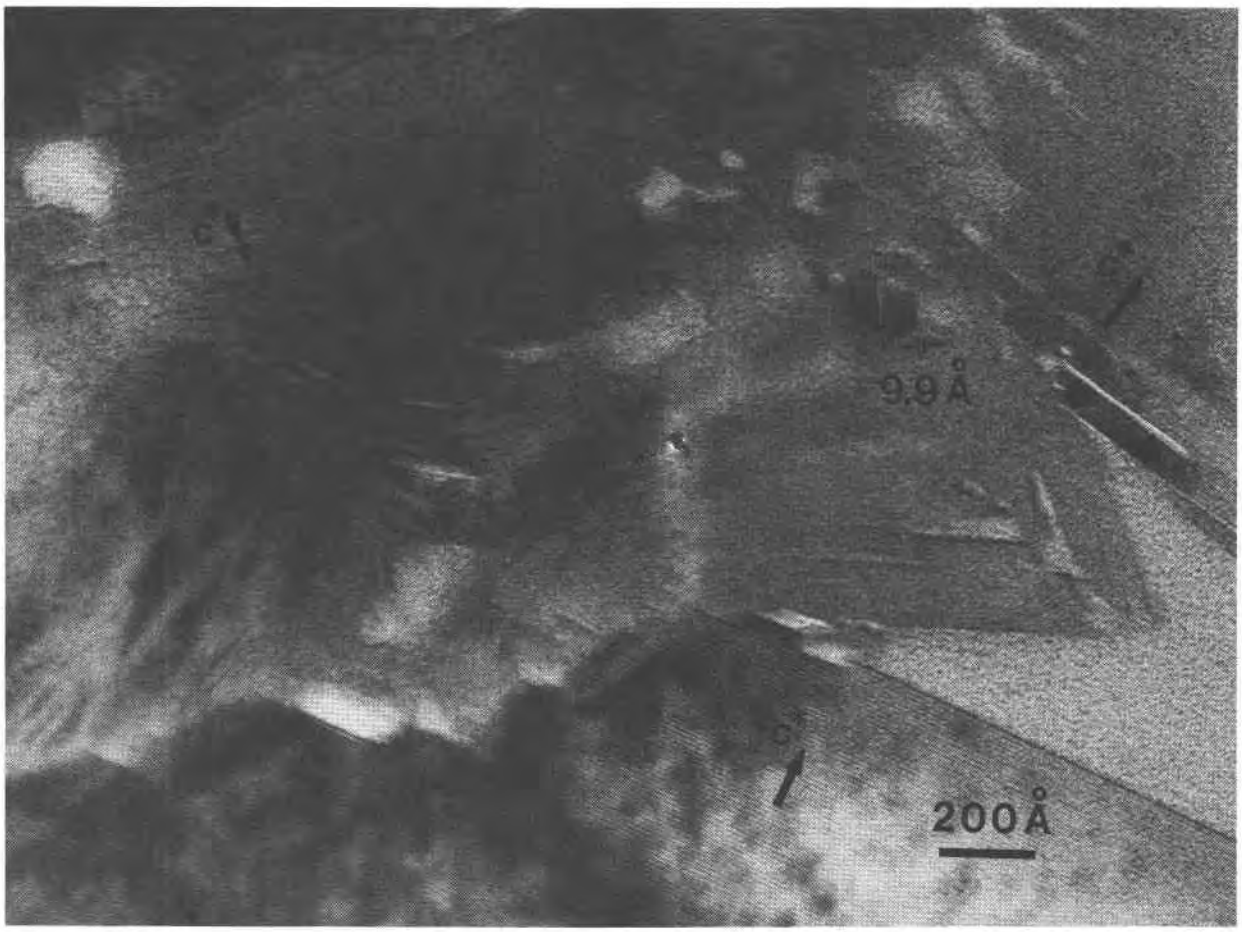

Fig. 13. Phengite grains showing a serrated boundary. Deformed phengites show kink-banding.

sity distribution of $8M_8$ shown by Ross et al. (1966), as shown schematically in Figures 11a and 11b. Some difference in the observed and theoretical patterns occurs insofar as some observed reflections in Figure 10b are shifted slightly or diffused about the central position. However, these features are not unexpected in that the stacking sequence is locally imperfect, and the selected area electron diffraction is obtained from an area much larger and more complex than that shown in Figure 10a.

Phengite deformation

One submicroscopic area of locally-deformed phengite was observed in a single sample, implying that such deformed phengite apparently is unusual. However, the TEM sample is itself a very small portion of the rock sample, and deformation may be more common than this one observation suggests. Phengite layers are bent and split into 100–500Å thick packets of layers that are complexly kinked (Fig. 12). Partially bent and split layers appear to be continuous with undeformed layers. Figure 13 shows the boundary between deformed and undeformed phengite from adjacent areas. The termination at the end of undeformed phengite layers has a serrated boundary, showing that this is due to brittle fracturing.

Deformation features in micas have been studied by several investigators using TEM techniques (e.g., Bell and Wilson, 1981; Knipe, 1981). Liewig et al. (1981) studied deformed phengite in the Schistes lustrés from the Northern Cottic Alps and observed that there are significant differences in Si content in phengite depending on the state of deformation. In our study qualitative AEM analyses show that there is no substantial difference between deformed and undeformed phengites, although deformed phengite may be slightly enriched in the minor elements Ti and Mn compared to the undeformed phengite. This may be due to original small differences in compositions of the areas selected for analysis, however. Because our samples exhibit no effects of post-deformation annealing, there is no reason to suspect that the deformation should give rise to composition differences.

The textural data imply that deformation postdated the metamorphic event that gave rise to equilibrium phases, and was not followed by a subsequent annealing event. These features collectively are consistent with high-presure

metamorphism of a subducted spilite initially forming micaeous eclogite gneiss. Subsequent local mechanical deformation of the micas without accompanying chemical changes may be related to cold deformation within the blueschist facies and/or during tectonic transport of the eclogite to the surface.

Conclusions

In the specimen studied, phengite lamellae commonly occur intergrown in paragonite at a scale below that of electron microprobe resolution and thus can cause difficulties in obtaining accurate single-phase chemical compositions. This kind of fine scale intergrowth of different micas may be common in both synthetic and natural micas. Great care should therefore be used in interpreting chemical analyses of micas. When data are suspect, structural and chemical characterization should be obtained with electron microscopy. Phengite in our samples is a highly structurally ordered, homogeneous phase, with Fe, Mg and other components randomly occurring in solid solutions.

Phengite and paragonite display more complex polytypic phenomena than initially expected, in part because powder X-ray diffraction patterns yield sharp, well-defined reflections. Separate grains of phengite are almost free of stacking disorder and consist of a well-ordered $2M_1$ polytype. However, paragonite shows more stacking disorder, a higher density of edge dislocations, and complex polytypism, including an 8-layer polytype.

Acknowledgments

We gratefully acknowledge constructive reviews by S. W. Bailey, M. Ross and D. R. Veblen. We wish to thank W. C. Bigelow, L. F. Allard, and D. F. Blake and the staff of the University of Michigan Electron Microbeam Analysis Laboratory for their efforts with respect to STEM facilities. We also thank J. H. Lee and L. M. Anovitz for assistance with AEM and electron microprobe analysis. This study was supported by NSF grant EAR-8313236 to D. R. Peacor.

References

Ahn, J. H. and Peacor, D. R. (1985) Transmission electron microscopic study of diagenetic chlorite in Gulf Coast argillaceous sediments. Clays and Clay Minerals, 33, 228–236.

Albee, A. L. and Chodos, A. A. (1965) Microprobe analysis of interlayered muscovite and paragonite, Lincoln Mountain Quadrangle, Vermont. (abstr.) Geological Society of America Bulletin, 78, 2.

Amouric, Marc and Baronnet, Alain (1983) Effect of early nucleation conditions on synthetic muscovite polytypism as seen by high resolution transmission electron microscopy. Physics and Chemistry of Minerals, 9, 146–159.

Amouric, Marc, Mercuriot, Geneviève and Baronnet, Alain (1981) On computed and observed HRTEM images of perfect mica polytypes. Bulletin de Minéralogie, 104, 298–313.

Bailey, S. W. (1980) Structures of layer silicates. In G. W. Brindley and G. Brown, Eds., Crystal Structures of Clay Minerals and Their X-ray Identification, p. 1–123. Mineralogical Society, London.

Banno, Shohei (1964) Petrologic studies on Sanbagawa crystalline schists in the Bessi-Ino district, Central Shikoku, Japan. Journal of the Faculty of Science, University of Tokyo, Sect. 2, v. 15, 203–319.

Baronnet, Alain (1975) Growth spirals and complex polytypism in micas: I. Polytypic structure generation. Acta Crystallographica, A31, 345–355.

Bell, I. A. and Wilson, C. J. L. (1981) Deformation of biotite and muscovite: TEM microstructure and deformation model. Tectonophysics, 78, 201–228.

Black, P. M. (1975) Mineralogy of New Caledonian metamorphic rocks: IV. Sheet silicates from the Ouégoa district. Contributions to Mineralogy and Petrology, 49, 269–284.

Blake, D. F., Allard, L. F., Peacor, D. R., and Bigelow, W. C. (1980) Ultra-clean X-ray spectra in the JEOL JEM-100CX. Proceedings of Electron Microscopic Society of America, 38, 136–137.

Blake, D. F. and Peacor, D. R. (1981) Biomineralization in crinoid echinoderms: characterization of crinoid skeletal elements using TEM and STEM microanalysis. Scanning Electron Microscopy, III, 321–328.

Blencoe, J. G. and Luth, W. C. (1973) Muscovite-paragonite solvi at 2, 4, and 8 kb pressure. (abstr.) Geological Society of America, Abstracts with Programs, 5, 553–554.

Brown, B. E. and Bailey, S. W. (1962) Chlorite polytypism: I. Regular and semi-random one-layer structure. American Mineralogist, 47, 819–850.

Brown, E. H. (1968) The Si^{4+} content of natural phengites: A discussion. Contributions to Mineralogy and Petrology, 17, 78–81.

Burnham, C. W. and Radoslovich, E. W. (1964) Crystal structures of coexisting muscovite and paragonite. Carnegie Institution of Washington Year Book, 63, 232–236.

Chiesa, S., Liborio, G., Mottana, A., and Pasquarè, G. (1972) La paragonite nei calcescisti delle apli: Distribuzione e interpretazione geopetrologica. Memorie della Società Geologica Italiana, 11, 1–30.

Cipriani, C., Sassi, F. P., and Bassani, C. V. (1968) La compozione delle miche chiare in rapporto con le constanti reticolari e col grado metamorphico. Rendiconti della Società Italiana di Mineralogica e Petrologica, 24, 3–37.

Coleman, R. G. and Lee, D. E. (1963) Glaucophane-bearing metamorphic rock types of the Cazadero area, California. Journal of Petrology, 4, 260–301.

Dudley, P. P. (1969) Electron microprobe analysis of garnet in glaucophane schists and associated eclogites. American Mineralogist, 54, 1139–1150.

Ernst, W. G. (1963) A note on phengitic micas from glaucophane schists. American Mineralogist, 48, 1357–1373.

Ernst, W. G. (1964) Petrological study of coexisting minerals from low-grade schists, Eastern Shikoku, Japan. Geochimica et Cosmochimica Acta, 28, 1631–1668.

Ernst, W. G. (1976) Mineral chemistry of eclogites and related rocks from the Voltri Group, Western Liguria, Italy. Schweizerische Mineralogische und Petrographische Mitteilungen, 56, 293–343.

Ernst, W. G. and Dal Piaz, G. V. (1978) Mineral paragenesis of eclogitic rocks and related mafic schists of the Piemonte ophiolite nappe, Breuil-St. Jacques area, Italian Western Alps. American Mineralogist, 63, 621–640.

Essene, E. J. (1967) Petrogenesis of Franciscan metamorphic rocks. Ph.D. thesis, University of California, Berkeley.

Essene, E. J. and Fyfe, W. S. (1967) Omphacite in California metamorphic rocks. Contributions to Mineralogy and Petrology, 15, 1–23.

Eugster, H. P. (1956) Muscovite–paragonite join and its use as a geological thermometer. (abstr.) Geological Survey of America Bulletin, 67, 1963.

Eugster, H. P., Albee, A. E., Bence, A. E., and Thompson, J. B. Jr. (1972) The two-phase region and excess mixing properties of paragonite–muscovite crystalline solutions. Journal of Petrology, 13, 147–179.

Eugster, H. P. and Yoder, H. S. Jr. (1955) The join muscovite–paragonite. Carnegie Institution of Washington Year Book, 54, 124–126.

Feininger, Thomas (1980) Eclogite and related high-pressure regional metamorphic rocks from the Andes of Ecuador. Journal of Petrology, 21, 107–140.

Foster, M. D. (1956) Correlation of dioctahedral potassium micas on the basis of their charge relations. U.S. Geological Survey Bulletin, 1036-D, 57–67.

Frey, Martin (1969) A mixed-layer paragonite–phengite of low-grade metamorphic origin. Contributions to Mineralogy and Petrology, 24, 63–65.

Frey, Martin, Hunziker, J. C., Jäger, E., and Stern, W. B. (1983) Regional distribution of white K-mica polymorphs and their phengite content in the Central Alps. Contributions to Mineralogy and Petrology, 83, 185–197.

Guidotti, C. V. (1968) On the relative scarcity of paragonite. American Mineralogist, 53, 963–974.

Güven, Nicep (1971) Structural factors controlling stacking sequences in dioctahedral micas. Clays and Clay Minerals, 19, 159–165.

Güven, Nicep and Burnham, C. W. (1967) The crystal structure of 3T muscovite. Zeitschrift für Kristallographie, 125, 163–183.

Heinrich, C. A. (1982) Kyanite–eclogite to amphibolite facies evolution of hydrous mafic and pelitic rocks, Adula nappe, Central Alps. Contributions to Mineralogy and Petrology, 81, 30–38.

Höck, Volker (1974) Coexisting phengite, paragonite and margarite in metasediments of the Mittlere Hohe Tauern, Austria. Contributions to Mineralogy and Petrology, 43, 261–273.

Holland, T. J. B. (1979) High water activities in the generation of high pressure kyanite eclogites of the Tauern Window, Austria. Journal of Geology, 87, 1–27.

Iijima, Sumio and Buseck, P. R. (1978) Experimental study of disordered mica structures by high-resolution electron microscopy. Acta Crystallographica, A34, 709–719.

Iijima, Sumio and Zhu, Jing (1982) Electron microscopy of a muscovite–biotite interface. American Mineralogist, 67, 1195–1205.

Iiyama, J. T. (1964) Étude des réactions d'échange d'ions Na-K dans la série muscovite-paragonite. Bulletin de la Société française de Minéralogie et de Cristallographie, 87, 532–541.

Katagas, Christos (1980) Ferroglaucophane and chloritoid-bearing metapelites from the phyllite series, Southern Peloponnese, Greece. Mineralogical Magazine, 43, 975–978.

Katagas, Christos and Baltatzis, E. (1980) Coexisting celadonitic muscovite and paragonite in chlorite zone metapelites. Neues Jahrbuch für Mineralogie, Monatshefte, 206–214.

Knipe, R. J. (1981) The interaction of deformation and metamorphism in slates. Tectonophysics, 78, 249–272.

Krogh, E. J. (1980) Geochemistry and petrology of glaucophane-bearing eclogites and associated rocks from Sunnfjord, Western Norway. Lithos, 13, 355–380.

Lee, J. H., Ahn, J. H., and Peacor, D. R. (1985) Textures in layer silicates: progressive changes through diagenesis and low temperature metamorphism. Journal of Sedimentary Petrology, 55, 532–540.

Liborio, G. and Mottana, A. (1975) White micas with 3T polymorph from the Calcescisti of the Alps. Neues Jahrbuch für Mineralogie, Monatschefte, 546–555.

Liewig, N., Caron, J., and Clauer, N. (1981) Geochemical and K-Ar isotopic behavior of Alpine sheet silicates during polyphased deformation. Tectonophysics, 78, 273–290.

Makanjuola, A. A. and Howie, R. A. (1972) The mineralogy of the glaucophane schists and associated rocks from Île de Groix, Brittany, France. Contributions to Mineralogy and Petrology, 35, 83–118.

Nicol, A. W. and Roy, Rustum (1965) Some observations on the system muscovite-paragonite. Canadian Journal of Earth Science, 2, 401–405.

Oberhänsli, R. (1980) *P–T* Bestimmungen anhand von Mineralanalysen in Eklogiten und Glaukophaniten der Ophiolite von Zermatt. Schweizerische Mineralogische und Petrographische Mitteilungen, 60, 215–235.

Olives Baños, Juan, Amouric, Marc, de Fouquet, Chantal, and Baronnet, Alain (1983) Interlaying and interlayer slip in biotite as seen by HRTEM. American Mineralogist, 68, 754–758.

Popov, A. A. (1968) Compositions of muscovites and paragonites synthesized at temperatures of 350–500°. Geokhimiya, 2, 131–144.

Powell, Roger and Evans, J. A. (1983) A new geobarometer for the assemblage biotite–muscovite–chlorite–quartz. Journal of Metamorphic Geology, 1, 331–336.

Radoslovich, E. W. and Norrish, K. (1962) The cell dimensions and symmetry of layer-lattice silicates: 1. Some structural considerations. American Mineralogist, 47, 559–616.

Rosenfeld, J. R., Thompson, J. B. Jr., and Zen, E-an (1958) Data on coexistent muscovite and paragonite. (abstr.) Geological Society of America Bulletin, 69, 1637.

Ross, Malcolm, Takeda, Hiroshi, and Wones, D. R. (1966) Mica polytypes: Systematic description and identification. Science, 151, 191–193.

Schaller, W. T. (1950) An interpretation of the composition of high silica sericites. Mineralogical Magazine, 29, 406–415.

Schreyer, Werner, Medenbach, O., Abraham, K., Gerbert, W., Müller, W. F. (1982) Kulkeite, a new metamorphic phyllosilicate mineral: Ordered 1:1 chorite/talc mixed-layer. Contributions to Mineralogy and Petrology, 80, 103–109.

Smith, J. V. and Yoder, H. S. Jr. (1956) Experimental and theoretical studies of the mica polymorphs. Mineralogical Magazine, 31, 209–331.

Stöckhert, B. (1985) Compositional control on the polymorphism ($2M_1$–3T) of phengitic white mica from high pressure parageneses of the Sesia Zone (lower Aosta valley, Western Alps; Italy). Contributions to Mineralogy and Petrology, 89, 52–58.

Takeda, Hiroshi and Ross, Malcolm (1975) Mica polytypism: Dissimilarities in the crystal structure of coexisting 1M and $2M_1$ biotite. American Mineralogist, 60, 1030–1040.

Veblen, D. R. (1980) Anthophyllite asbestos: microstructures, intergrown sheet silicates and mechanisms of fiber formation. American Mineralogist, 65, 1075–1086.

Veblen, D. R. (1983a) Exsolution and crystal chemistry of the sodium mica wonesite. American Mineralogist, 68, 554–565.

Veblen, D. R. (1983b) Microstructures and mixed layering in intergrown wonesite, chlorite, talc, biotite and kaolinite. American Mineralogist, 68, 566–580.

Veblen, D. R. and Buseck, P. R. (1979) Serpentine minerals: intergrowths and new combination structures. Science, 206, 1398–1400.

Veblen, D. R. and Buseck, P. R. (1980) Microstructures and reac-

tion mechanisms in biopyriboles. American Mineralogist, 65, 599–623.

Veblen, D. R. and Buseck, P. R. (1981) Hydrous pyriboles and sheet silicates in pyroxenes and uralites: intergrowth microstructures and reaction mechanism. American Mineralogist, 66, 1107–1134.

Veblen, D. R. and Ferry, J. M. (1983) A TEM study of the biotite-chlorite reaction and comparison with petrologic observations. American Mineralogist, 68, 1160–1168.

Velde, Bruce (1965a) Experimental determination of muscovite polymorph stabilities. American Mineralogist, 50, 436–449.

Velde, Bruce (1965b) Phengite micas: Synthesis, stability and natural occurrence. American Journal of Science, 263, 886–913.

Velde, Bruce (1967) Si^{4+} content of natural phengites. Contributions to Mineralogy and Petrology, 14, 250–258.

Velde, Bruce (1970) Les éclogites de la région nantaise (de Campbon au Cellier, Loire-Atlantique). Bulletin de la Société française de Minéralogie et de Cristallographie, 93, 370–385.

Yau, T. C., Anovitz, L. M., Essene, E. J., and Peacor, D. R. (1984) Phlogopite-chlorite reaction mechanism and physical conditions during retrograde reaction in the Marble Formation, Franklin, New Jersey. Contributions to Mineralogy and Petrology, 88, 299–306.

Zen, E-an and Albee, A. L. (1964) Coexistent muscovite and paragonite in pelitic schists. American Mineralogist, 49, 904–925.

Manuscript received, April 24, 1984;
accepted for publication, July 2, 1985.